Case 16976

Eurorad

Cerebral oligodendroglioma

Published on 26.08.2020

ISSN: 1563-4086
Section: Neuroradiology
Area of Interest: CNS Oncology
Imaging Technique: CT
Imaging Technique: MR
Case Type: Clinical Cases
Authors: Jesper Dierickx1,2, Philippe Bernard[2], Dimitri De Vuyst[2], Filip Vanhoenacker1,2,3
Patient: 31 years, female

Clinical History:

A 31-year-old woman presents with a new-onset seizure.

Imaging Findings:

Non-enhanced CT (Fig. 1) shows a low density in the left frontal lobe with cortical sulcal effacement. There are intralesional hyperdense foci, compatible with calcifications, and a central area with fluid attenuation, corresponding with cyst formation. There is midline shift and subfalcine herniation to the right side. There is no contrast enhancement (Fig. 1).

MRI shows increased signal of the left frontal lobe on T2-WI and FLAIR sequences (Fig. 2). On T1 MPRAGE sequences, the lesion is hypointense, with effacement of cortical sulci. There are no susceptibility artefacts on T2* sequences. The lesion shows no contrast enhancement after IV administration of gadolinium nor diffusion restriction. The cystic changes in the centre of the lesion are confirmed. Histopathologic examination of the biopsy specimen confirms an oligodendroglioma. Genetic analysis demonstrates a 1p/19q co-deletion.

Discussion:

Oligodendroglioma is a glial tumour and is characterised by a 1p/19q co-deletion, which differentiates the lesion from other glial tumors [1]. It usually affects adults between 40 and 60 years old [2]. Epileptic seizures are the most common initial presentation, with or without generalisation [3].

On CT, oligodendroglioma usually presents as a hypodense mass, predominantly with a cortical-subcortical location, but it can be of heterogeneous density. It typically has a supratentorial location, most commonly in the frontal lobe [2,4]. Intratumoral calcification is present in about 90% of cases [2]. Cystic formation and haemorrhage are not frequent [2,5]. The lesion is hypointense on T1-WI and heterogeneous hyperintense on T2-WI. Subtle, multifocal enhancement is present in about 50%.

Oligodendrogloma shows no diffusion restriction. On perfusion imaging, it may show elevated relative cerebral blood volume (rCBV). Moderately elevated choline (Cho) and decreased N-acetylaspartate (NAA) without a lactate peak is seen on MR spectroscopy [2,6].

The differential diagnosis of epilepsy-associated tumors with calcifications include gangliogliomas, dysembryoplastic neuroepithelial tumours (DNET), pleomorphic xanthoastrocytomas (PXA) and low-grade diffuse astrocystomas. Ganglioglioma can be either predominantly solid or predominantly cystic, and is usually located in the mesial temporal lobe [7,8]. DNETs are typically multicystic cortical-based lesions, commonly located in the mesial temporal or frontal lobe [5,9]. PXAs are cortical-based cystic tumours with a solid, mural component and leptomeningeal enhancement [8]. The most common location is the temporal lobe (49%) [7]. In low-grade diffuse astrocytoma, cortical involvement is typically absent [2].

Ganglioglioma, DNET and PXA typically occur in younger patients than an oligodendroglioma. Intralesional calcification are rarely present in low-grade diffuse astrocytoma, PXA and DNET and in about 40% of gangliogliomas. Compared to oligodendroglioma, cystic formation is more prominent and frequent in DNET and PXA. However, these imaging features are insufficient to reliably distinguish oligodendroglioma from other epilepsy-associated tumors [5,7,8].

Therefore, biopsy is mandatory to confirm the diagnosis. Treatment requires a multi-disciplinary approach. Surgical resection reduces mass effect and symptoms, delays progression and improves survival. Both chemotherapy and radiotherapy may be considered [6]. Oligodendroglioma has a better prognosis than glial tumours without 1p/19q co-deletion, with a median survival of 14 years after chemoradiotherapy. However, in most patients, the final outcome is infaust [10].

In conclusion, a cortical-subcortical-based mass in the frontal lobe with intralesional calcification in patients between the age of 40- 60 years presenting with epilepsy is suggestive of an oligodendroglioma. Histological confirmation is required for final diagnosis.

Written informed patient consent for publication has been obtained.

Differential Diagnosis List: Oligodendroglioma, Ganglioglioma, DNET, PXA, Low-grade diffuse astrocytoma

Final Diagnosis: Oligodendroglioma

References:

Lapointe S, Perry A, Butowski NA (2018). Primary brain tumours in adults. Lancet. 392:432–46 (PMID:30060998).
Smits M (2016). Imaging of oligodendroglioma. Br J Radiol. 89:20150857 (PMID:26849038).
Jooma R, Waqas M, Khan I (2019). Diffuse Low-Grade Glioma - Changing Concepts in Diagnosis and Management: A Review. Asian J Neurosurg. 14:356–63 (PMID:31143247).
Behin A, Hoang-Xuan K, Carpentier AF, Delattre J-Y (2003). Primary brain tumours in adults. Lancet. 361:323–31 (PMID: 12559880).
Luzzi S, Elia A, Del Maestro M, Elbabaa SK, Carnevale S, Guerrini F, Caulo M, Morbini P, Galzio R (2019). Dysembryoplastic Neuroepithelial Tumors: What You Need to Know. World Neurosurg. 127:255–65 (PMID: 30981794).
Jenkinson MD, Walker C, Brodbelt AR, Wilkins S, Husband D, Haylock B (2010). Molecular genetics, imaging and treatment of oligodendroglial tumours. Acta Neurochir. 152:1815–25 (PMID:20811757).
Koeller KK, Henry JM (2001). From the archives of the AFIP: superficial gliomas: radiologic-pathologic correlation. Radiographics. 21:1533–56 (PMID: 11706224).
Friedman E (2014). Epilepsy imaging in adults: Getting it right. Am J Roentgenol. 203:1093–103 (PMID:25341150).
Urbach H (2005). Imaging of the epilepsies. Eur Radiol. 15:494–500 (PMID:15678321).
Van Den Bent MJ, Bromberg JEC, Buckner J (2016). Low-grade and anaplastic oligodendroglioma. In: Berger MS, Weller M. Handbook of Clinical Neurology. Elsevier B.V. 134:361–80. (PMID:26948366).

Figure 1

a

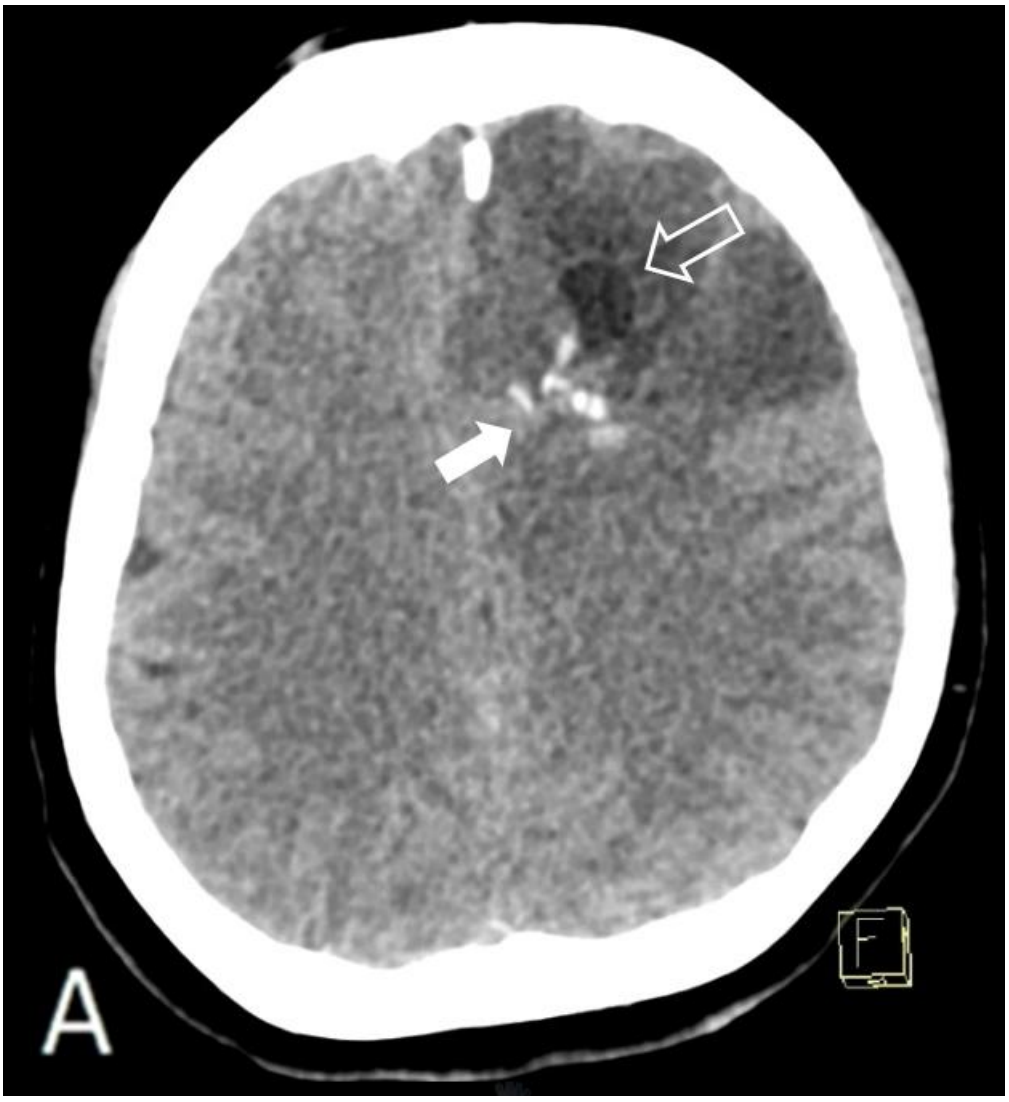

Description: Non-enhanced and enhanced CT. Axial and coronal non-enhanced CT images (a, b, c, d) show a low density in the left frontal lobe with cortical sulcal effacement, coarse intralesional calcifications (white arrow) and a central cyst formation (void arrow). There is midline shift and subfalcine herniation to the contralateral side. On axial contrast-enhanced CT images (e, f), there is no contrast enhancement. **Origin:** © Department of Radiology, Algemeen Ziekenhuis Sint-Maarten, Mechelen, Belgium,2020

b

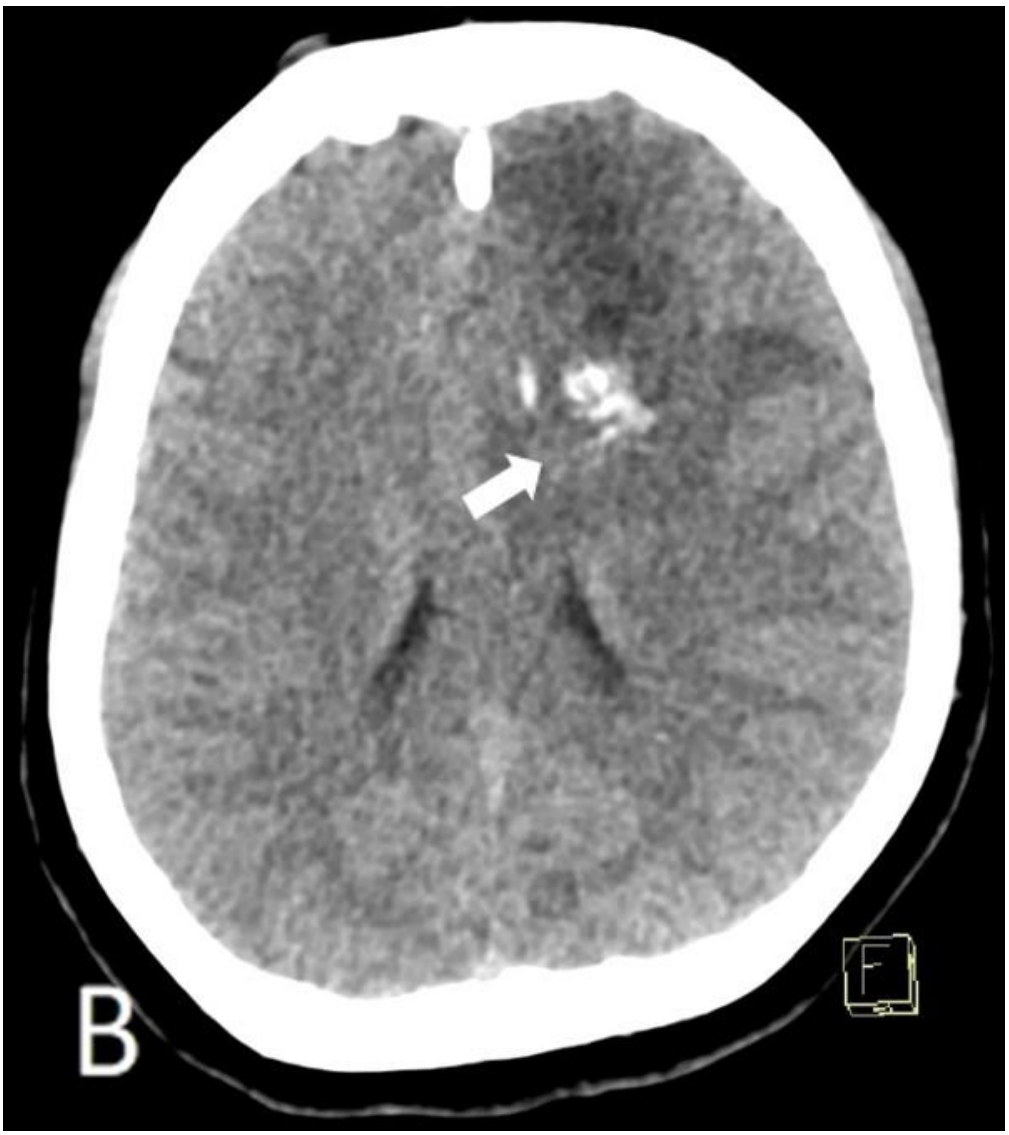

Description: Non-enhanced and enhanced CT. Axial and coronal non-enhanced CT images (a, b, c, d) show a low density in the left frontal lobe with cortical sulcal effacement, coarse intralesional calcifications (white arrow) and a central cyst formation (void arrow). There is midline shift and subfalcine herniation to the contralateral side. On axial contrast-enhanced CT images (e, f), there is no contrast enhancement. **Origin:** © Department of Radiology, Algemeen Ziekenhuis Sint-Maarten, Mechelen, Belgium,2020

c

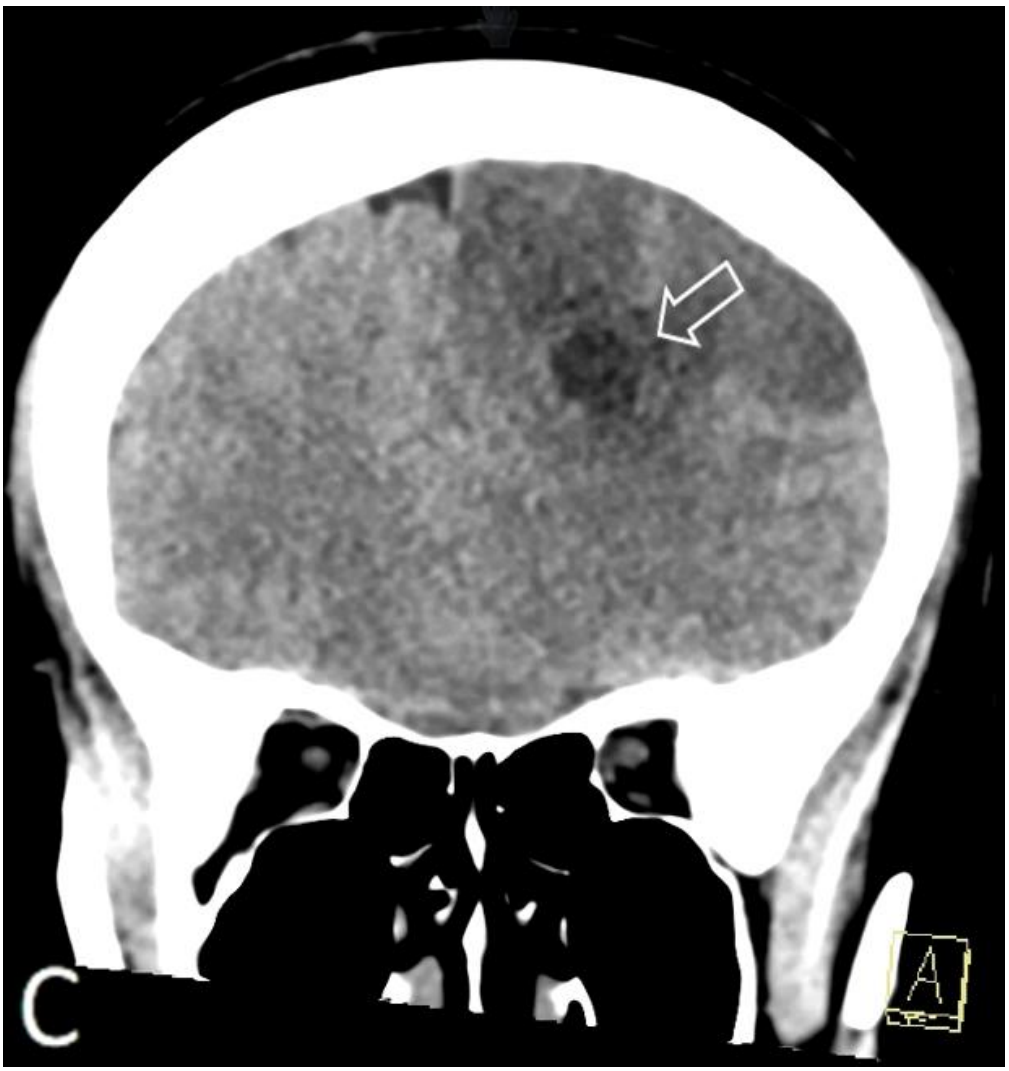

Description: Non-enhanced and enhanced CT. Axial and coronal non-enhanced CT images (a, b, c, d) show a low density in the left frontal lobe with cortical sulcal effacement, coarse intralesional calcifications (white arrow) and a central cyst formation (void arrow). There is midline shift and subfalcine herniation to the contralateral side. On axial contrast-enhanced CT images (e, f), there is no contrast enhancement. **Origin:** © Department of Radiology, Algemeen Ziekenhuis Sint-Maarten, Mechelen, Belgium,2020

d

Description: Non-enhanced and enhanced CT. Axial and coronal non-enhanced CT images (a, b, c, d) show a low density in the left frontal lobe with cortical sulcal effacement, coarse intralesional calcifications (white arrow) and a central cyst formation (void arrow). There is midline shift and subfalcine herniation to the contralateral side. On axial contrast-enhanced CT images (e, f), there is no contrast enhancement. **Origin:** © Department of Radiology, Algemeen Ziekenhuis Sint-Maarten, Mechelen, Belgium,2020

e

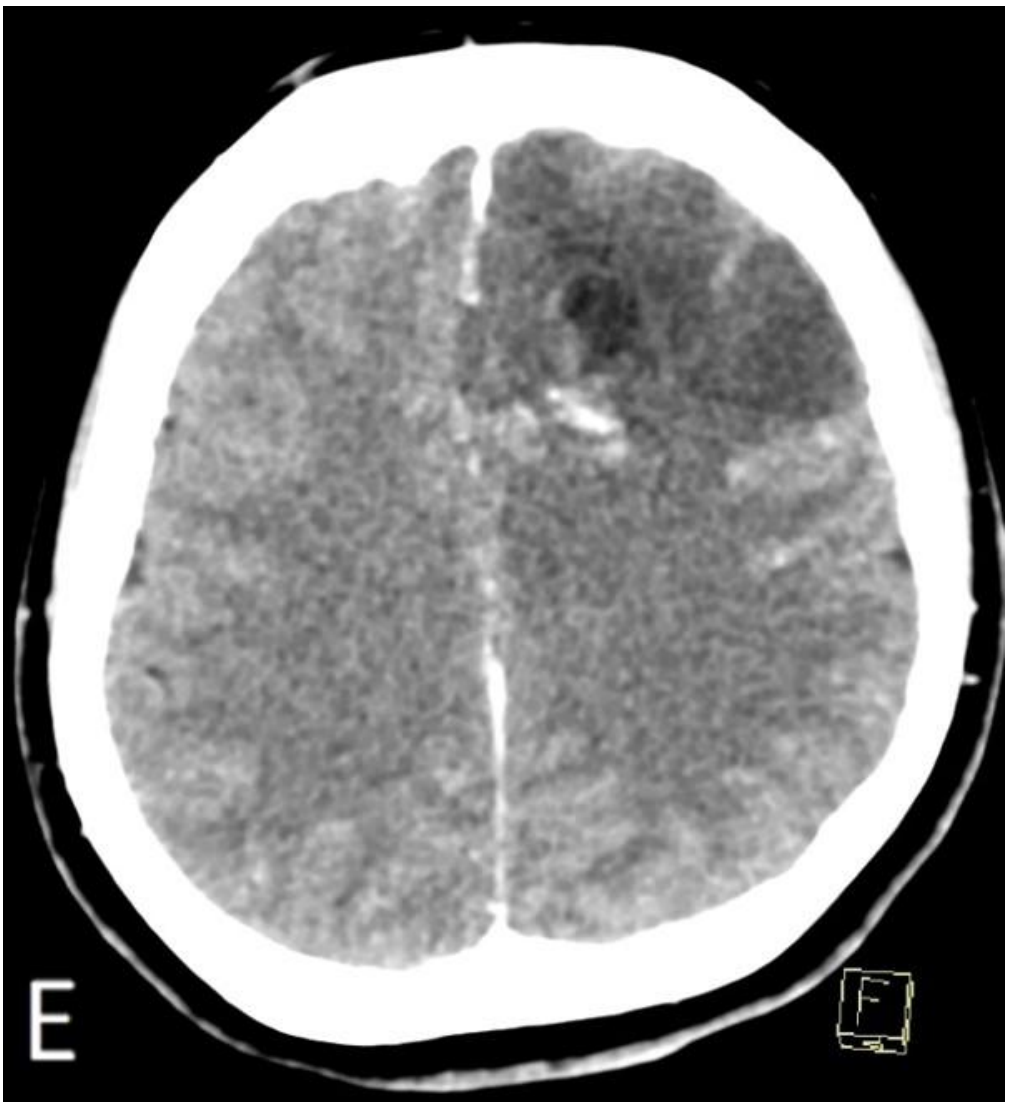

Description: Non-enhanced and enhanced CT. Axial and coronal non-enhanced CT images (a, b, c, d) show a low density in the left frontal lobe with cortical sulcal effacement, coarse intralesional calcifications (white arrow) and a central cyst formation (void arrow). There is midline shift and subfalcine herniation to the contralateral side. On axial contrast-enhanced CT images (e, f), there is no contrast enhancement. **Origin:** © Department of Radiology, Algemeen Ziekenhuis Sint-Maarten, Mechelen, Belgium,2020

f

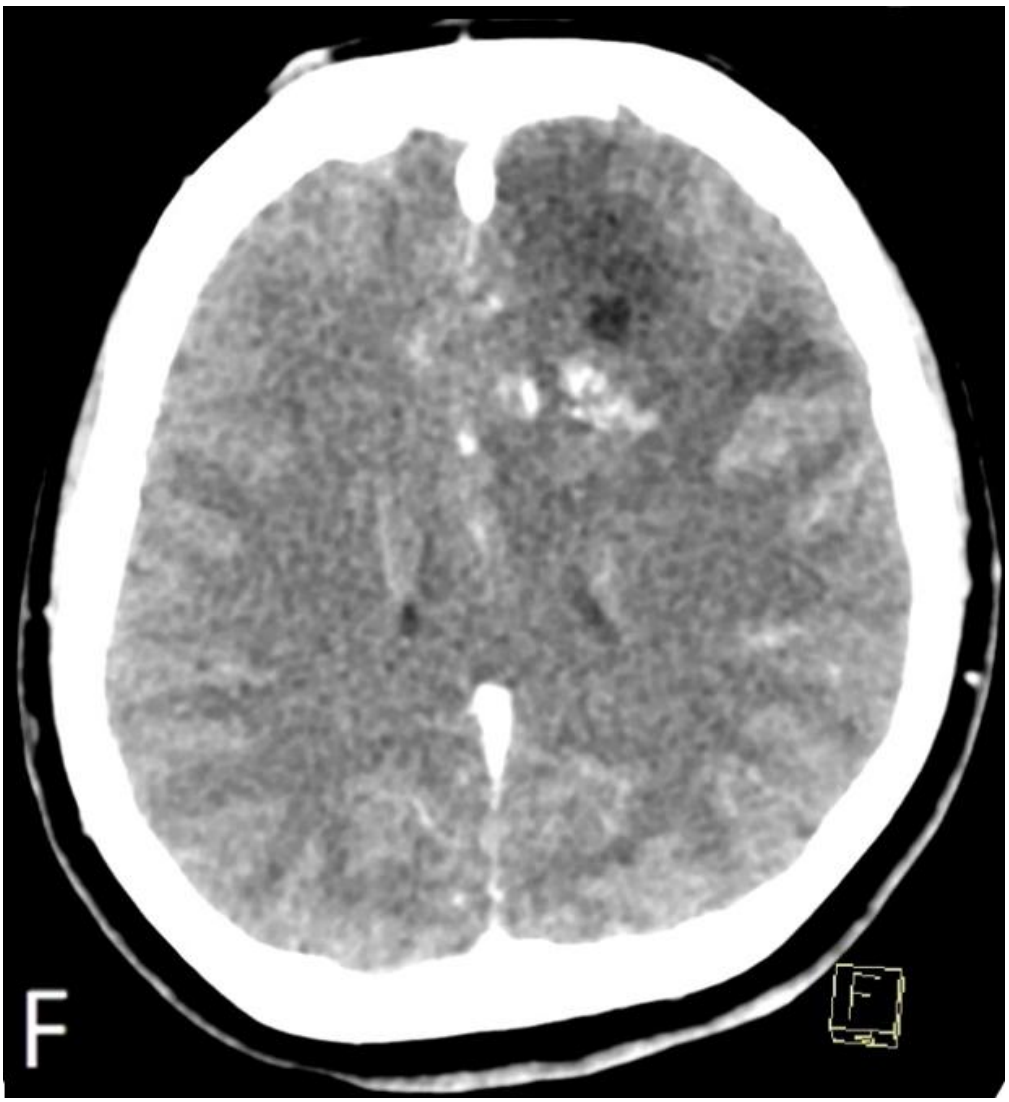

Description: Non-enhanced and enhanced CT. Axial and coronal non-enhanced CT images (a, b, c, d) show a low density in the left frontal lobe with cortical sulcal effacement, coarse intralesional calcifications (white arrow) and a central cyst formation (void arrow). There is midline shift and subfalcine herniation to the contralateral side. On axial contrast-enhanced CT images (e, f), there is no contrast enhancement. **Origin:** © Department of Radiology, Algemeen Ziekenhuis Sint-Maarten, Mechelen, Belgium,2020

Figure 2

a

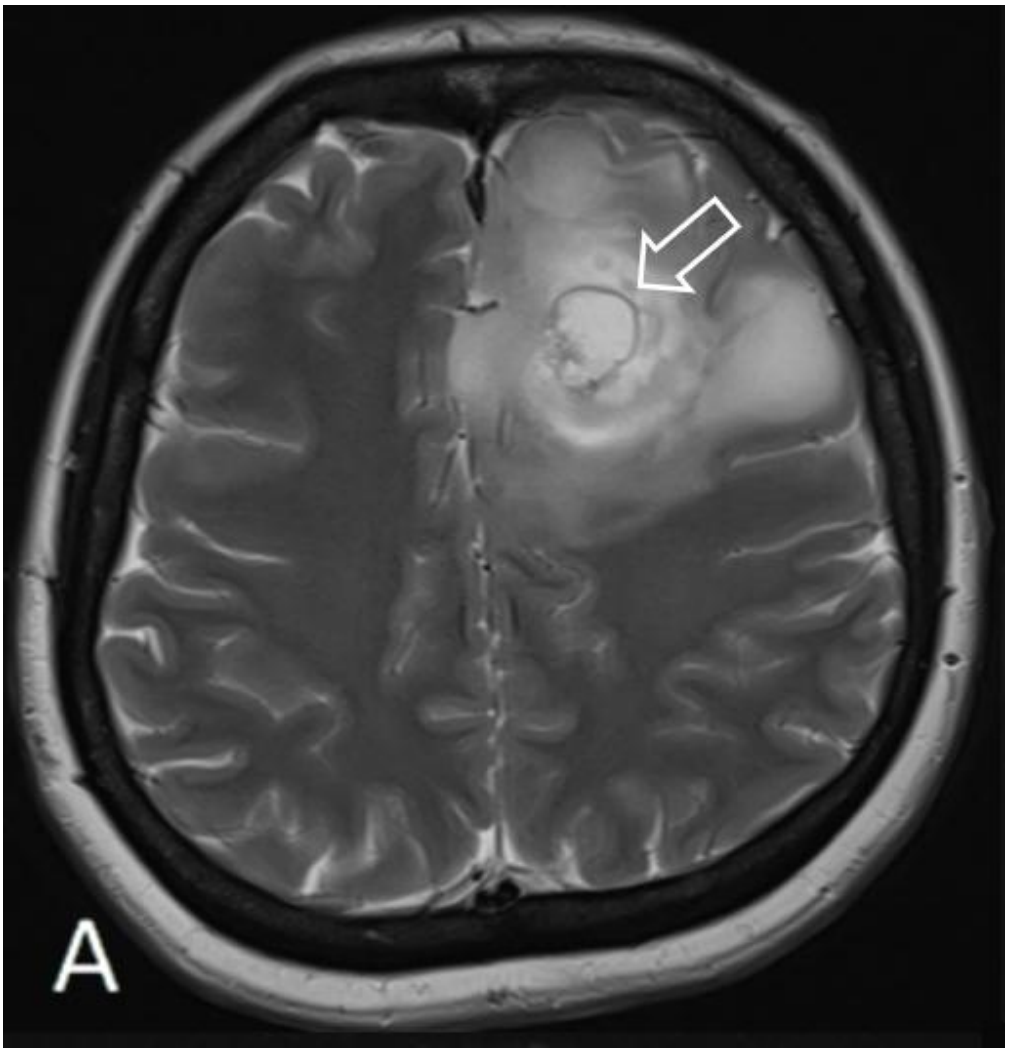

Description: MRI. Axial T2-WI (a) and axial FLAIR images (b) demonstrate increased signal in the left frontal lobe with a centrally located cyst (void arrow). Axial T1 MPRAGE sequence (c) shows decreased corticomedullary differentiation in the left frontal lobe with a centrally located cyst (void arrow). Axial T2* images (d) show absence of susceptibility artefact. No significant contrast enhancement on axial contrast-enhanced T1 MPRAGE images (e) and subtraction images (f). Axial B1000 diffusion-weighted images (g) with ADC-mapping (h) show no diffusion restriction. **Origin:** © Department of Radiology, Algemeen Ziekenhuis Sint-Maarten, Mechelen, Belgium,2020

b

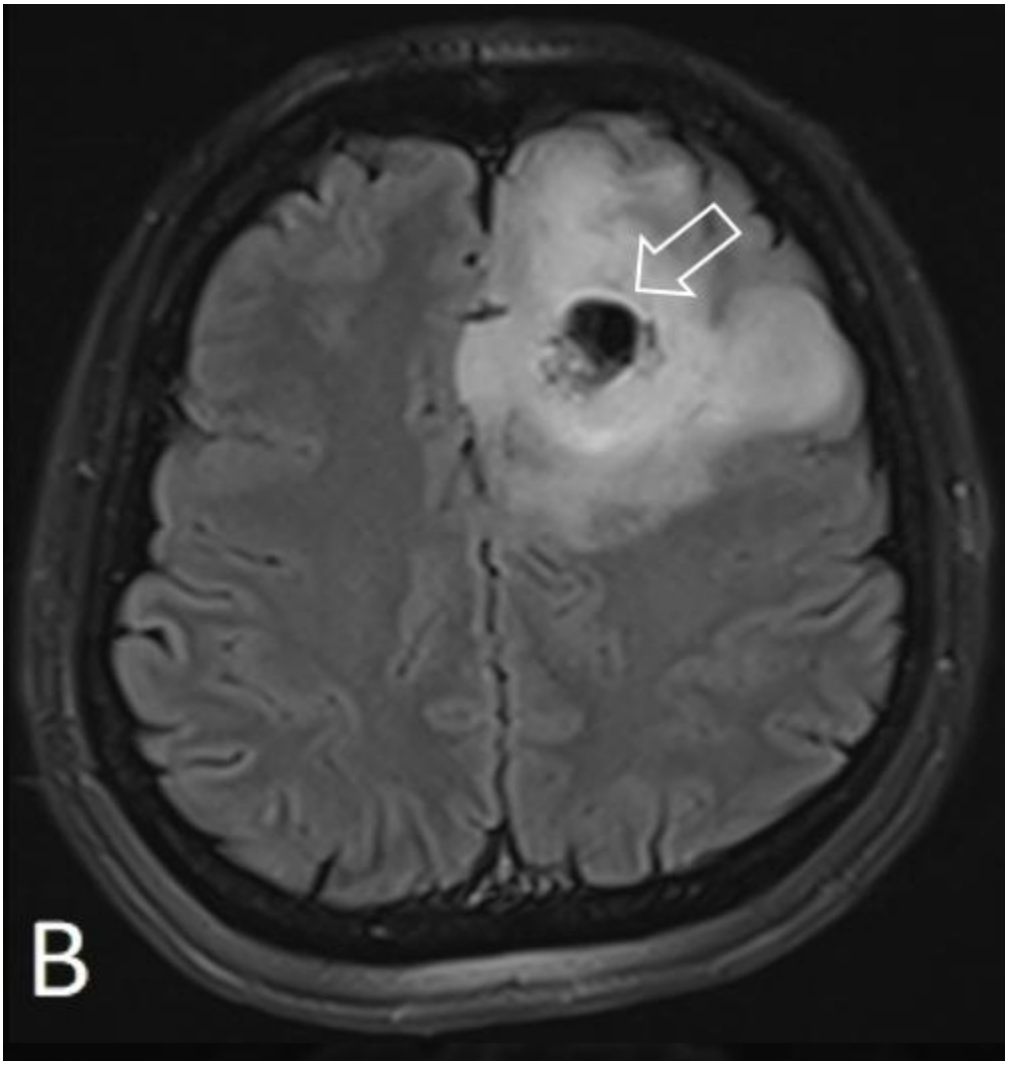

Description: MRI. Axial T2-WI (a) and axial FLAIR images (b) demonstrate increased signal in the left frontal lobe with a centrally located cyst (void arrow). Axial T1 MPRAGE sequence (c) shows decreased corticomedullary differentiation in the left frontal lobe with a centrally located cyst (void arrow). Axial T2* images (d) show absence of susceptibility artefact. No significant contrast enhancement on axial contrast-enhanced T1 MPRAGE images (e) and subtraction images (f). Axial B1000 diffusion-weighted images (g) with ADC-mapping (h) show no diffusion restriction. **Origin:** © Department of Radiology, Algemeen Ziekenhuis Sint-Maarten, Mechelen, Belgium,2020

c

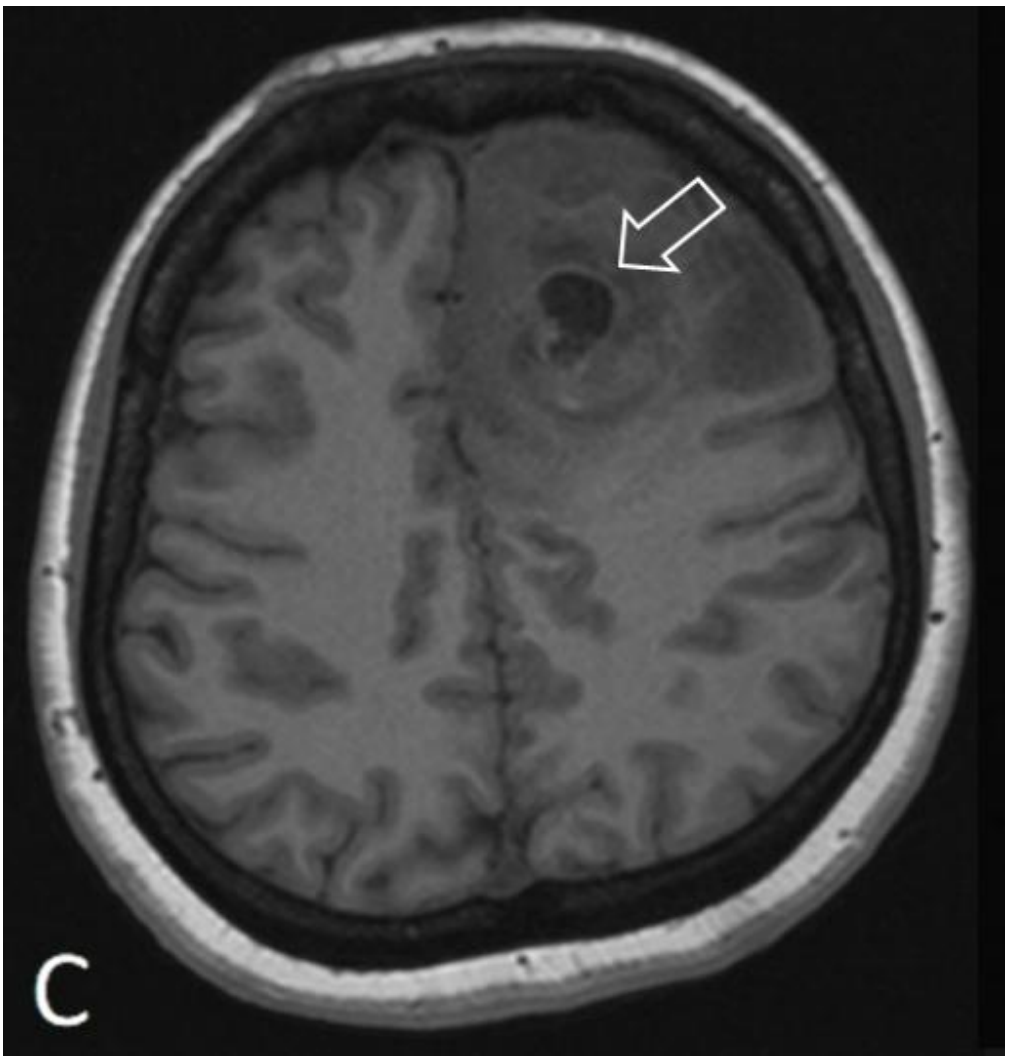

Description: MRI. Axial T2-WI (a) and axial FLAIR images (b) demonstrate increased signal in the left frontal lobe with a centrally located cyst (void arrow). Axial T1 MPRAGE sequence (c) shows decreased corticomedullary differentiation in the left frontal lobe with a centrally located cyst (void arrow). Axial T2* images (d) show absence of susceptibility artefact. No significant contrast enhancement on axial contrast-enhanced T1 MPRAGE images (e) and subtraction images (f). Axial B1000 diffusion-weighted images (g) with ADC-mapping (h) show no diffusion restriction. **Origin:** © Department of Radiology, Algemeen Ziekenhuis Sint-Maarten, Mechelen, Belgium,2020

d

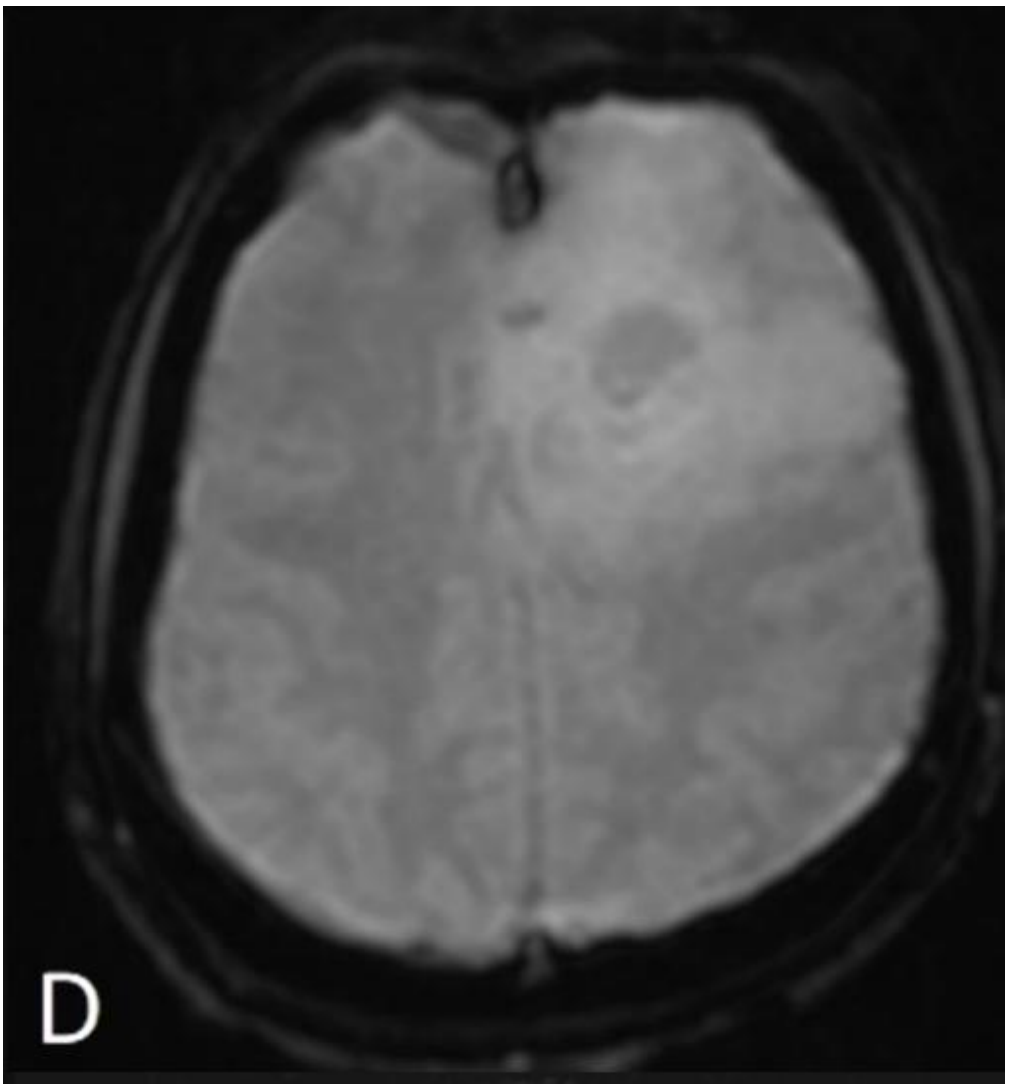

Description: MRI. Axial T2-WI (a) and axial FLAIR images (b) demonstrate increased signal in the left frontal lobe with a centrally located cyst (void arrow). Axial T1 MPRAGE sequence (c) shows decreased corticomedullary differentiation in the left frontal lobe with a centrally located cyst (void arrow). Axial T2* images (d) show absence of susceptibility artefact. No significant contrast enhancement on axial contrast-enhanced T1 MPRAGE images (e) and subtraction images (f). Axial B1000 diffusion-weighted images (g) with ADC-mapping (h) show no diffusion restriction. **Origin:** © Department of Radiology, Algemeen Ziekenhuis Sint-Maarten, Mechelen, Belgium,2020

e

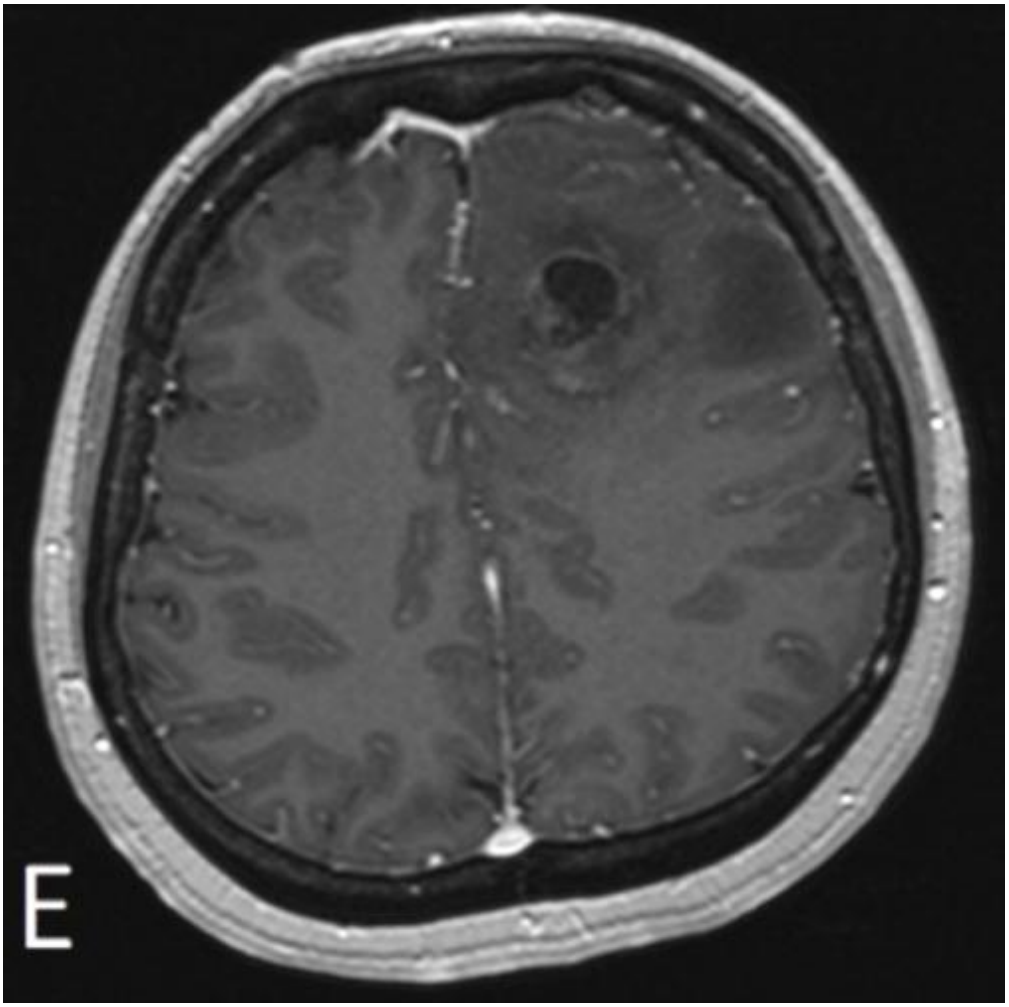

Description: MRI. Axial T2-WI (a) and axial FLAIR images (b) demonstrate increased signal in the left frontal lobe with a centrally located cyst (void arrow). Axial T1 MPRAGE sequence (c) shows decreased corticomedullary differentiation in the left frontal lobe with a centrally located cyst (void arrow). Axial T2* images (d) show absence of susceptibility artefact. No significant contrast enhancement on axial contrast-enhanced T1 MPRAGE images (e) and subtraction images (f). Axial B1000 diffusion-weighted images (g) with ADC-mapping (h) show no diffusion restriction. **Origin:** © Department of Radiology, Algemeen Ziekenhuis Sint-Maarten, Mechelen, Belgium,2020

f

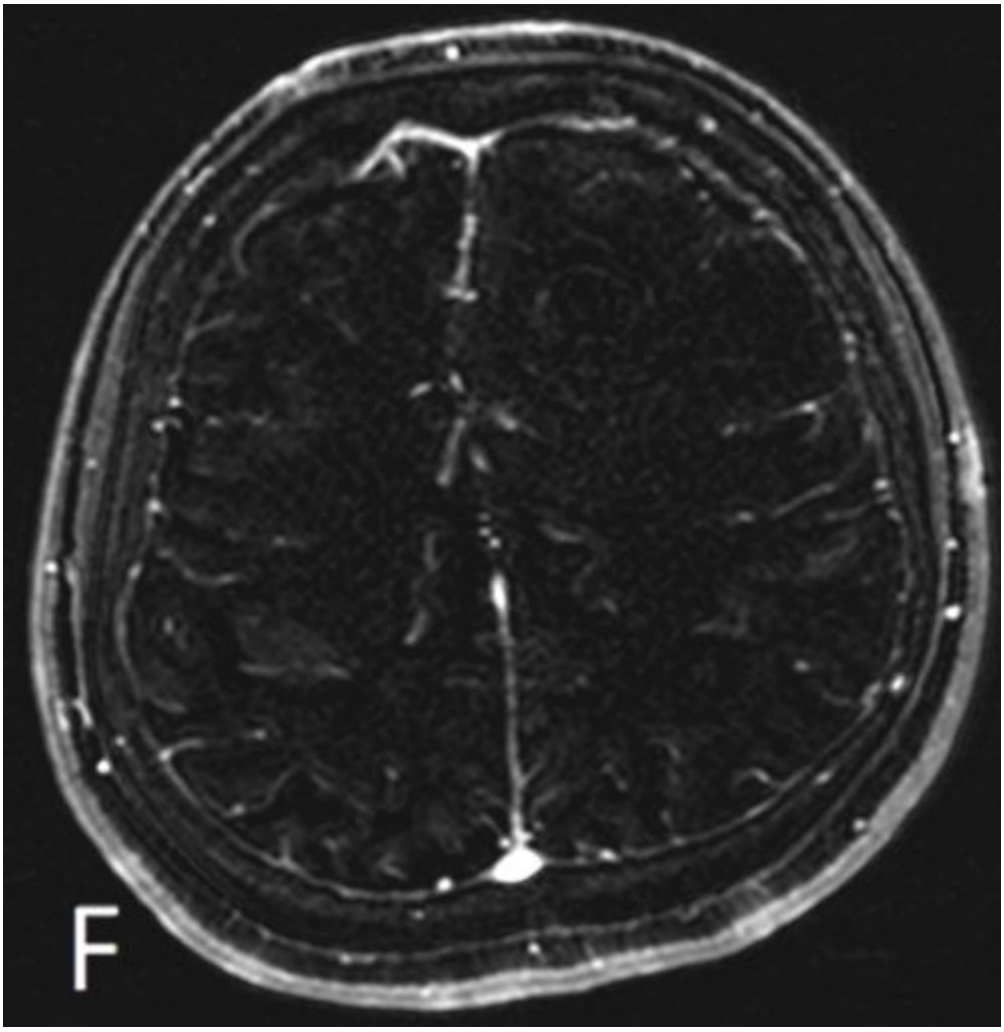

Description: MRI. Axial T2-WI (a) and axial FLAIR images (b) demonstrate increased signal in the left frontal lobe with a centrally located cyst (void arrow). Axial T1 MPRAGE sequence (c) shows decreased corticomedullary differentiation in the left frontal lobe with a centrally located cyst (void arrow). Axial T2* images (d) show absence of susceptibility artefact. No significant contrast enhancement on axial contrast-enhanced T1 MPRAGE images (e) and subtraction images (f). Axial B1000 diffusion-weighted images (g) with ADC-mapping (h) show no diffusion restriction. **Origin:** © Department of Radiology, Algemeen Ziekenhuis Sint-Maarten, Mechelen, Belgium,2020

g

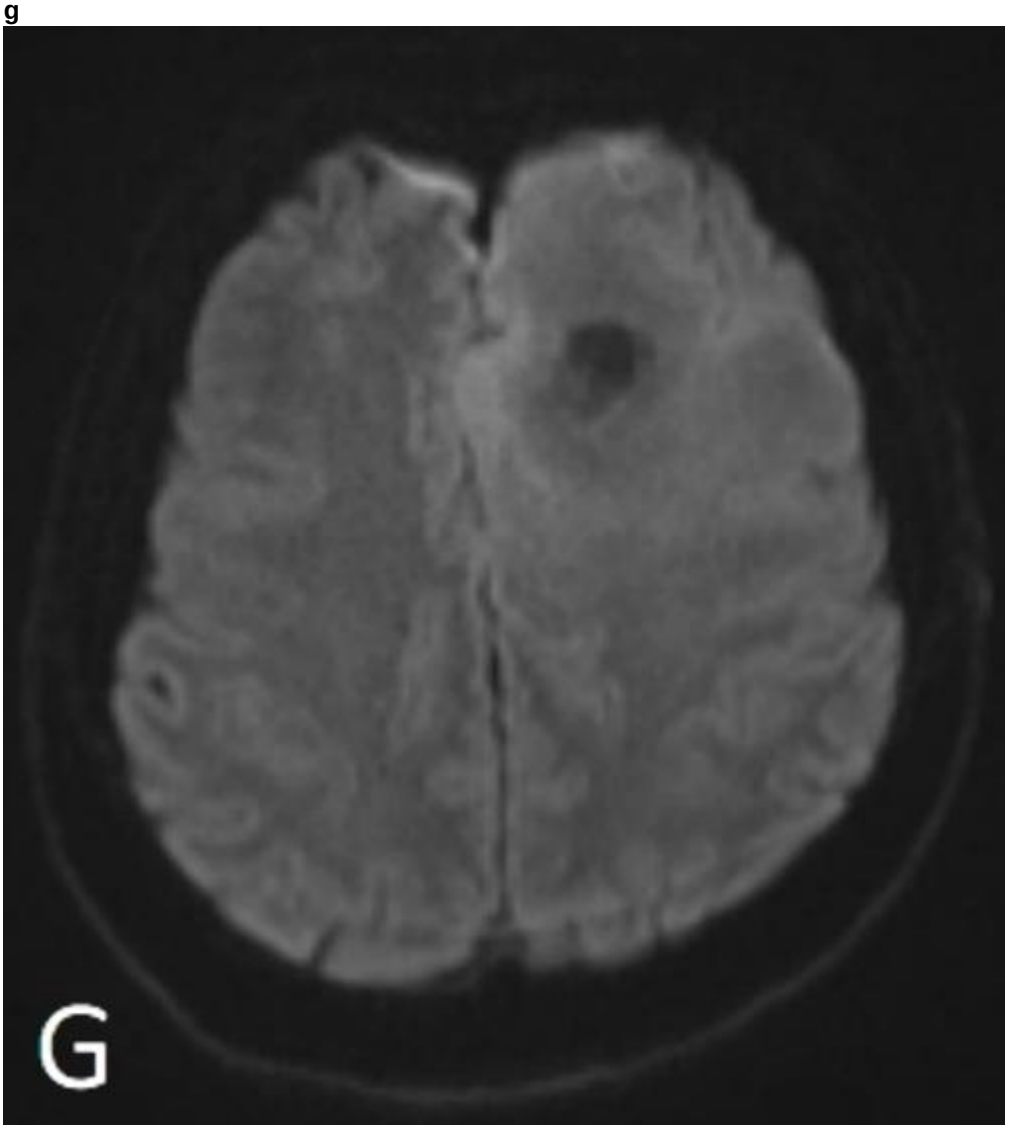

Description: MRI. Axial T2-WI (a) and axial FLAIR images (b) demonstrate increased signal in the left frontal lobe with a centrally located cyst (void arrow). Axial T1 MPRAGE sequence (c) shows decreased corticomedullary differentiation in the left frontal lobe with a centrally located cyst (void arrow). Axial T2* images (d) show absence of susceptibility artefact. No significant contrast enhancement on axial contrast-enhanced T1 MPRAGE images (e) and subtraction images (f). Axial B1000 diffusion-weighted images (g) with ADC-mapping (h) show no diffusion restriction. **Origin:** © Department of Radiology, Algemeen Ziekenhuis Sint-Maarten, Mechelen, Belgium,2020

h

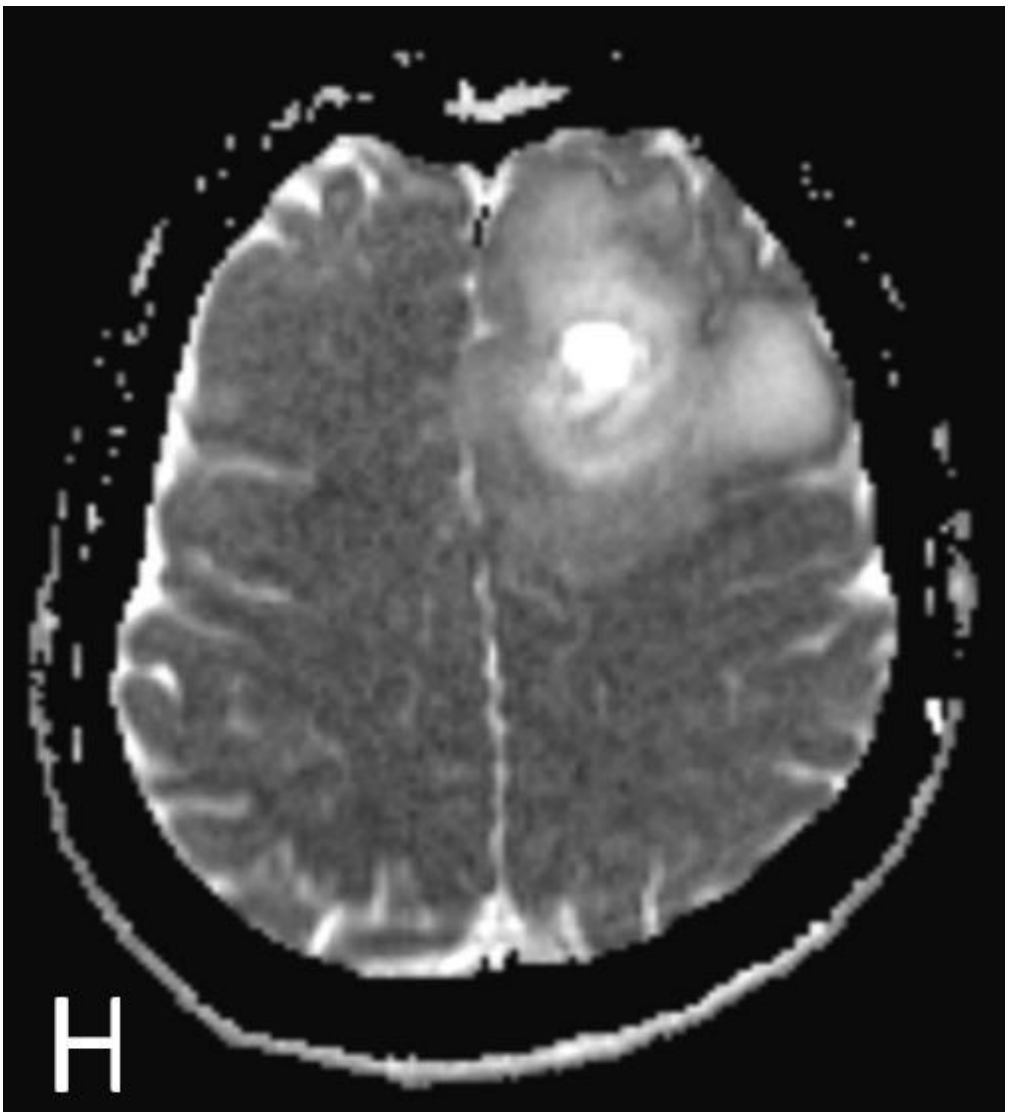

Description: MRI. Axial T2-WI (a) and axial FLAIR images (b) demonstrate increased signal in the left frontal lobe with a centrally located cyst (void arrow). Axial T1 MPRAGE sequence (c) shows decreased corticomedullary differentiation in the left frontal lobe with a centrally located cyst (void arrow). Axial T2* images (d) show absence of susceptibility artefact. No significant contrast enhancement on axial contrast-enhanced T1 MPRAGE images (e) and subtraction images (f). Axial B1000 diffusion-weighted images (g) with ADC-mapping (h) show no diffusion restriction. **Origin:** © Department of Radiology, Algemeen Ziekenhuis Sint-Maarten, Mechelen, Belgium,2020